INTERNATIONAL JOURNAL OF HYDROGEN ENERGY 40 (2015) 3822–3837

Available online at www.sciencedirect.com

ScienceDirect

journal homepage: www.elsevier.com/locate/he

Dynamic operation and feasibility study of a self-sustainable hydrogen fueling station using renewable energy sources

*Li Zhao, Jacob Brouwer**

Advanced Power and Energy Program, University of California, Irvine, CA 92697-3550, USA

ARTICLE INFO

Article history:
Received 18 October 2014
Received in revised form
12 January 2015
Accepted 12 January 2015
Available online 14 February 2015

Keywords:
Renewable hydrogen
Hydrogen fueling station
Electrolyzer
Fuel cell
Dynamics

ABSTRACT

To evaluate the dynamic operation and feasibility of designing and operating a self-sustainable hydrogen fueling station using renewable energy sources, dynamic system models have been developed for a hydrogen fueling station utilizing a proton exchange membrane (PEM) electrolyzer and fuel cell. Using fueling and power demand data from an existing public hydrogen station in Irvine, California, dynamic analyses of the self-sustainable station have been carried out. Various control strategies are developed and evaluated to determine the impacts of control strategies and renewable capacity factors on the efficiency and other performance characteristics of the station. The simulation results and analysis suggest that with careful sizing and system design, a self-sustainable hydrogen fueling station that relies completely upon renewable sources for hydrogen production, storage and dispensing is feasible. Moreover, a cost and sensitivity analysis is carried out to evaluate the levelized hydrogen cost for different station designs. The cost of the hydrogen is determined to be as low as $6.71 per kg or $9.14 per kg when the station is powered by 200 kW of wind turbines or 360 kW of PV arrays, respectively.

Introduction

Over the next decade, a transition is expected to occur in the transportation sector as combustion automobiles fueled by gasoline are gradually shifting to electric drive trains. In this transition, hydrogen powered fuel cell vehicles are playing important roles. Automakers have made remarkable advances in the development of fuel cell vehicles and are projecting initial commercialization in the 2015–2017 timeframe [1]. As a promising alternative fuel for transportation, hydrogen enables electric vehicle operation with rapid fueling, long range, and large vehicle zero emissions features, which cannot be provided by any other zero-emissions transportation technology [2–4]. As of the year 2013, there are a total of 58 hydrogen fueling stations in the U.S. including private stations. Most of these fueling stations are constructed to support demonstration and research projects that will initiate the further development of hydrogen infrastructure and provide important insights to accelerate the introduction of hydrogen fuel cell vehicles to the market. With higher market penetration of hydrogen fuel cell vehicles in the near future, hydrogen fueling infrastructure must be introduced to meet the increasing demand.

* *Corresponding author*. Tel.: +1 949 824 1999x221; fax: +1 949 824 7423.
E-mail address: jb@apep.uci.edu (J. Brouwer).
http://dx.doi.org/10.1016/j.ijhydene.2015.01.044

Nomenclature

F	Faraday constant, 96,485 C mol^{-1}
R	gas constant, 8.3144 J K^{-1} mol^{-1}
η_{act}	activation overpotential, V
η_{ohm}	ohmic overpotential, V
η_{diff}	diffusion overpotential, V
z	number of electrons transferred
P_{H_2}	partial pressures of hydrogen
P_{O_2}	partial pressures of oxygen
P_{H_2O}	partial pressures of water
α	transfer coefficient
i_0	exchange current density, A cm^{-2}
i_{0_A}	anode exchange current density, A cm^{-2}
i_{0_C}	cathode exchange current density, A cm^{-2}
δ_m	thickness of the membrane, cm
A	membrane cross-sectional area, cm^2
σ_m	conductivity of the proton exchange membrane, S cm^{-1}
λ_E	degree of humidification of the membrane
r_m	resistivity of the proton exchange membrane, Ω cm
λ_{FC}	water content of the membrane
T	temperature, K

Hydrogen can be produced from various sources via diverse pathways with different levels of emissions associated with each approach [5]. Renewable hydrogen produced by the electrolysis of water with electricity derived from renewable energy sources could potentially eliminate the green-house-gas and air pollutant emissions [5–7] from fuel production and delivery. In addition, as fossil fuel reserves are depleted over the years, renewable fuel provision will become increasingly important for transportation sustainability. Therefore hydrogen fueling stations powered by renewable energy sources will not only achieve zero-emission hydrogen production and support California requirements for 33% renewable hydrogen (California Senate Bill 1505), but could also significantly extend the existing network of hydrogen fueling stations to the remote areas.

For the purpose of investigating the feasibility of a self-sustainable hydrogen fueling station powered by renewable energy sources, dynamic system models have been developed to simulate the renewable sources and fueling dynamics together with hydrogen production and station operation. Theoretical models have been integrated to simulate station performance when subjected to measured power and fueling demand dynamics from a public fueling station and measured renewable energy supply dynamics (wind and solar). The theoretical models that are integrated into various self-sustainable station design configurations include a Proton Exchange Membrane (PEM) electrolyzer and fuel cell, wind turbines, hydrogen compressor, and hydrogen storage tank. The wind speed and solar PV power output are measured from real wind farms and PV installations, respectively. The hydrogen fueling station power consumption and hydrogen fueling dynamic profiles are measured from the public hydrogen fueling station at the University of California, Irvine. Detailed analyses are carried out to evaluate various control strategies to determine station efficiency, effects on capacity factors of the renewable sources, sizing analysis of the renewables, and the levelized hydrogen cost estimation and sensitivity to various parameters. This study presents a dynamic model and representative results for designing, sizing, evaluating and controlling a self-sustainable renewable hydrogen fueling station.

A variety of experimental and simulation studies have been carried out to advance hydrogen fueling technology and to facilitate the deployment of hydrogen infrastructure. Such studies have been mainly focused upon [8]: 1) improving electrolysis technology to accommodate renewable hydrogen production, 2) advancing hydrogen storage technology, 3) improving hydrogen production pathways and reducing costs, 4) analyzing and optimizing stand-alone hydrogen production and storage systems, and 5) addressing placement, safety issues, and regulatory policy.

Brown et al. [1] presented a successful public hydrogen fueling station at the University of California, Irvine, that has robustly and safely dispensed 25,000 kg of fuel over the course of 5 years. The average hydrogen consumption is 0.7 kg/car/day and the net station electric use is 5.18 kWh/kg. The net hydrogen cost is also reported to be $14.95 per kg of hydrogen. Farzaneh-Gord et al. [9] carried out a theoretical analysis investigating the performance of hydrogen fueling stations with different types of hydrogen storage technologies. Two storage types were compared and the results showed that the cascade storage type has many advantages over the buffer storage system. In their study, the optimized dimensionless low and medium-pressure reservoir pressures were identified. Shah et al. [10] presented a conceptual design of a solar powered hydrogen fueling station for a single family home. Sixty high-efficiency PV panels with a total capacity of 18.9 kW account for approximately 94.7% of the hydrogen home's power consumption. The fueling station consists of 1) a 165 bar high pressure electrolyzer for on-site production of 2.24 kg/day of hydrogen, 2) a three-bank cascade configuration of storage tanks and 3) a hydrogen dispensing nozzle. The system produces 0.8 kg/day of hydrogen for a fuel cell vehicle with an average daily commute of 56 km. The study evaluated the energy efficiency when incorporating a solar-hydrogen system for residential applications. Kelly et al. [7] reported the design and performance of a solar hydrogen fueling station at Milford, MI, which was comprised of high-efficiency PV modules, and a high-pressure (44.8 MPa) electrolyzer. In this system, direct connection between the PV and electrolyzer systems was proposed and optimized. The study showed that the electrolyzer operated efficiently on solar power over a wide range of conditions. More interestingly, occasional rapidly changing solar radiation and harsh weather conditions did not degrade the system performance [7]. This study estimated that the system could produce approximately 0.5 kg of high-pressure hydrogen per day on solar power for an average summer day in the Detroit area. Dagdougui et al. [11] developed a model combining a network of renewable hydrogen fueling stations and several renewable source nodes. The mathematical model determined the selection of renewable sources for the stations based upon distance and population density criteria, as well as the energy and

hydrogen flows exchanged among the system components from the production nodes to the demand points. Rothuizen et al. [12] established a thermodynamic model to simulate a high pressure hydrogen fueling station paired with a vehicle storage system. Properties such as pressure, temperature and mass flow were analyzed, and the results showed that the pressure loss in the hydrogen storage system has a significant impact on the hydrogen refueling process in terms of mass flow, cooling demand and storage dimensioning. It also suggested that the cascade fueling configuration reduces compressor work and cooling capacity significantly. Gahleitner [13] described 41 realized and seven planned power-to-gas systems and evaluated their operating experience with alkaline and PEM electrolyzers and fuel cells. Issues including system design, efficiency and lifetime, and potential regarding the integration of power-to-gas plants into current infrastructure are discussed. Princerichard et al. [14] developed a model to determine the key technical and economic parameters influencing the competitive position of decentralized electrolytic hydrogen production. The capital, maintenance and energy costs of water electrolysis, as well as a monetary valuation of the associated greenhouse gas (GHG) emissions were incorporated in the study. Electrolytic hydrogen was found to be commercially viable in some areas with relatively low electricity prices, and the hydrogen storage technology used was determined to be the most important technical issue. Gibson and Kelly [15] optimized the efficiency of a PV-electrolysis system by matching the voltage and maximum power output of the photovoltaics to the operating voltage of PEM electrolyzers. The hydrogen generation efficiency can be increased to 12% for a solar powered PV-PEM electrolyzer that can supply enough hydrogen to operate a fuel cell vehicle. Calderon et al. [16] described an exergy analysis of the energy behavior of the components of a hybrid photovoltaic-wind system with hydrogen storage. The study determined the exergy efficiency of the various components of the system, and calculated the exergy losses that occurred as a result of irreversibility. Harrison et al. [17] reported the design, installation, and operation of the Wind-to-Hydrogen (Wind2H2) project, in which hydrogen is produced directly from renewable energy sources. This project used solar and wind energy to produce and store hydrogen. Electrolyzer system efficiency was measured for both the PEM and alkaline electrolyzer technologies at various stack current levels. The report suggested that implementation of complete renewable electrolysis systems will require systems level design and integration.

Deshmukh and Boehm [18] provided a detailed review on renewable driven hydrogen systems and modeling approaches applicable to these systems that have been reported over the last two decades. Renewable energy sources, including solar photovoltaic, wind, and hydro, were summarized as the power sources in these reports; the options for hydrogen storage were also summarized. This review particularly emphasized aspects of modeling of the various components for the renewable hydrogen system. Carapellucci and Giordano [19] developed a simulation tool for evaluating energy and economic performance of renewable energy islands, including various electricity generation technologies (photovoltaic modules, wind turbines and micro-hydroelectric plants), integrated with a hydrogen storage system comprising an electrolyzer, a hydrogen storage tank and a fuel cell. The unit cost of energy was evaluated for grid-connected and stand-alone systems. A hybrid genetic-simulated annealing algorithm was used for system optimization. Dursun et al. [6] developed a model to simulate an electrolyzer using the electrical energy from a renewable energy system based on fundamental thermodynamics and empirical electrochemical relationships. In this study, hydrogen production capacity of a stand-alone renewable hybrid power system was evaluated and the results of the proposed model were calculated and compared with experimental data. However, the hydrogen tank and hydrogen compressors were omitted from this proposed dynamic model. Awasthi et al. [20] developed a PEM electrolyzer model in Matlab/Simulink to capture the dynamic behavior. The model was comprised of four blocks – anode, cathode, membrane and voltage, and model results showed operating temperature and pressure have opposite effects on the electrolyzer performance. Ohmic overpotential increases sharply with current density indicating improvement in performance is possible by using a low resistance electrolyte. Marangio et al. [21] reported results from both the theoretical and experimental points of view on a high pressure PEM electrolyzer stack. A theoretical model based on electrochemical equations was developed and validated by the experimental data. Some important process parameters were obtained and estimated for various temperature and pressure conditions. Maclay et al. [22–24] developed a dynamic model of a photovoltaic (PV) powered residence in a stand-alone configuration. The model assessed the sizing, capital costs, control strategies, and efficiencies of reversible fuel cells, batteries, and ultra-capacitors when used individually or in combination as hybrid hydrogen energy storage devices.

In terms of cost and safety issues, Saur et al. [25,26] of the National Renewable Energy Laboratory (NREL) described a hydrogen production cost analysis on a collection of optimized central wind-based water electrolysis production facilities. The study was part of NREL's Wind2H2 project that characterized the technical and economic implications of a large-scale wind electrolysis system. It showed that the cost of renewable wind-based hydrogen production is very sensitive to the cost of the wind electricity and the hydrogen costs ranged from $3.72/kg to $12.16/kg. Kim et al. [27] developed a 3D simulation of hydrogen leak scenario cases at a hydrogen fueling station. Four scenarios of a hydrogen explosion at a hydrogen fueling station were simulated based upon real geometrical configurations. The simulation results were validated with hydrogen jet experimental data to examine the diffusion behavior of a leaked hydrogen jet stream. A set of marginally safe configurations for fueling facility systems were presented.

As summarized above, studies have been carried out to investigate renewable hydrogen production/storage/dispense systems both experimentally and theoretically. However, few of these published studies have addressed the design and dynamic operation of a self-sustainable hydrogen fueling station that considers both renewable source dynamics and fueling dynamics, as in this effort. This study investigates the impacts of renewable power source dynamics coupled to

fueling station demand dynamics on overall renewable hydrogen fuel station system performance.

Method

As discussed in the previous section, there has been significant attention and interest in the hydrogen refueling station application and station placement. A self-sustainable hydrogen fueling station could provide better interconnections to the existing 'cluster' station approach. This work expands upon current understanding of various wind/solar-hydrogen systems and analyses on the dynamics associated with both renewable sources and hydrogen dispatching/fueling operations. This work also addresses the design and evaluation of control strategies used to size components and operate the renewable hydrogen fueling station. Furthermore, renewable hydrogen fuel costs for such self-sustainable station designs and operating dynamics are estimated in this study.

To analyze the feasibility and implications of a self-sustainable hydrogen fueling station using only renewable energy sources, a detailed dynamic system model comprised of renewable energy sources (wind turbine/solar PV) together with hydrogen production, compression, storage and dispatch components, is developed in MATLAB/Simulink®. The theoretical models that are integrated into various self-sustainable station design configurations include a PEM electrolyzer and fuel cell, wind turbines, hydrogen compressor, and hydrogen storage tank. The wind speed and solar PV power output are measured from real wind farms and PV installations. The hydrogen fueling station power consumption and hydrogen fueling dynamic profiles are measured from the public hydrogen fueling station at the University of California, Irvine. The performance of a renewable energy source in combination with a PEM electrolyzer and fuel cell, hydrogen compression, storage and dispensing system, form the basis of comparison amongst the various control strategies and operating conditions.

A schematic of a self-sustainable hydrogen fueling station using renewable sources modeled in this work is presented in Fig. 1. In the self-sustainable hydrogen fueling station, renewable energy from the wind turbine or solar PV is directed to the PEM electrolyzer that electrochemically splits water into hydrogen and oxygen gases. The hydrogen is compressed and stored in the storage tank for fueling or supplying power to the station. When power is required to meet the station load demand dynamics, either the stored hydrogen is converted back to electrical energy in a PEM fuel cell, or the renewable power is utilized directly, depending upon renewable power availability and the control strategy implemented. The oxygen byproduct is not utilized in this study, but it could also be collected and utilized for various applications. As shown in Fig. 1, the public hydrogen fueling station configuration at the University of California, Irvine includes 35 MPa and 70 MPa fueling and a refrigeration unit that were modeled in this study.

System description

Wind power model

Wind power was modeled using wind speed data with ten minute resolution, which was obtained from the Wind Integration Datasets of the National Renewable Energy Laboratory and 3TIER [28], and the detailed wind power model that is described by Zhao et al. [8]. Wind data obtained in 2006 comprised the primary input data set for the current simulations. In addition, three weeks of data, acquired from 6/30/2006 to 7/6/2006 (capacity factor = 0.41), 2/6/2006 to 2/12/2006 (capacity factor = 0.3) and 8/31/2006 to 9/6/2006 (capacity

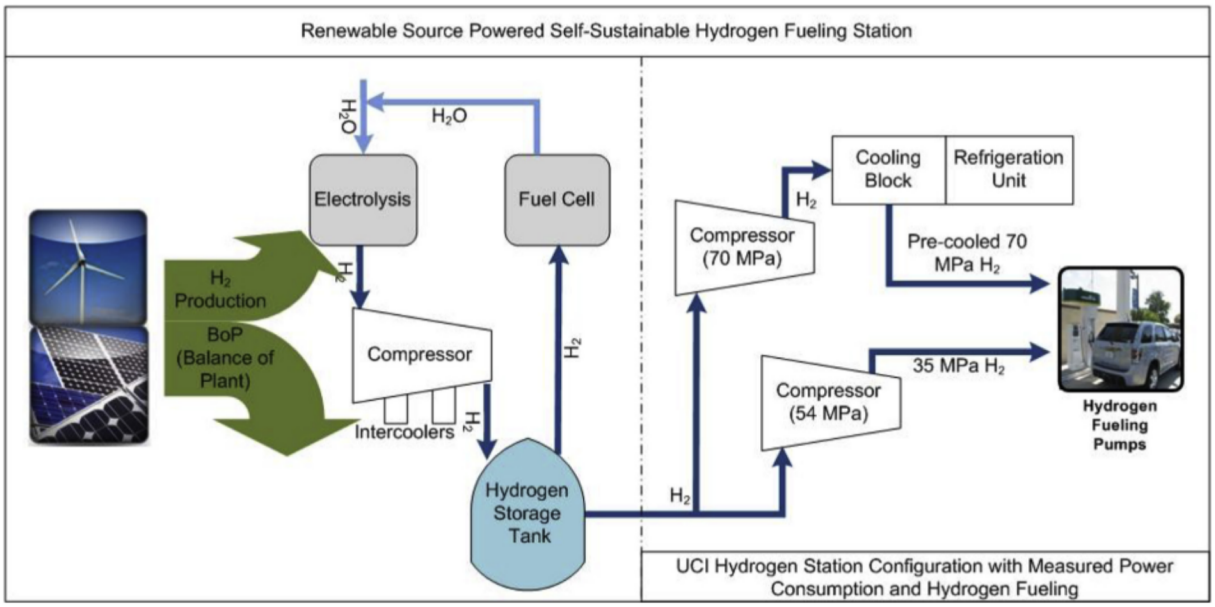

Fig. 1 – Schematic of a self-sustainable hydrogen fueling station.

factor = 0.2), comprised the input data set for the capacity factor sensitivity analyses.

Measured solar photovoltaic power output

The dynamic data for PV power output (kW vs. time (s)) were determined by measurement of a Unisolar 6 kW nominal DC amorphous PV array installed at the University of California, Irvine (latitude: 33.6 N, longitude: 117.7 W), on a time interval of every 15 min, 24 h/day [8,22,23]. Solar PV power output data obtained in 2001 comprised the primary input data set for the simulation presented in this study. Three weeks of data, acquired from 8/2/2001 to 8/8/2001 (capacity factor = 0.22), 3/21/2001 to 3/27/2001 (capacity factor = 0.14) and 2/22/2001 to 2/28/2001 (capacity factor = 0.06), comprised the primary input data set for the capacity factor sensitivity analyses. In addition, sensitivity to the insolation available at various locations was analyzed by considering a case of installation in the Mojave Desert.

Measured hydrogen fueling station power demand and hydrogen dispensed

Hydrogen fueling station power demand was obtained from the public hydrogen fueling station that has been in operation in Irvine, California since 2003. Station electricity consumption was measured as a function of hydrogen dispensed over a week period from 11/4/2012 to 11/10/2012. During this period, 24 kg of hydrogen were dispensed. Current was measured with 30 s resolution at the three-phase, 208 V feed line to the UCI hydrogen station and integrated to give electrical energy for all station loads [1]. The hydrogen station electrical load and the hydrogen dispensed over the week were shown in Figs. 2 and 3.

PEM electrolyzer model

The PEM electrolyzer physical model developed in this study was a steady-state model that simulates relationships between the cell voltage and cell current that account for activation losses, diffusion losses, and ohmic losses in a PEM electrolyzer

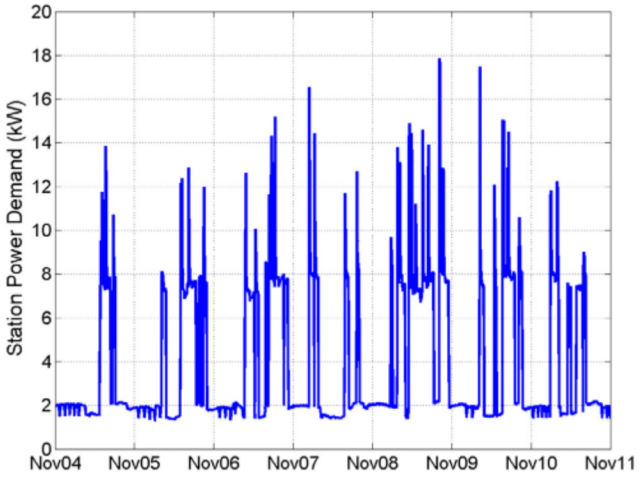

Fig. 2 – UCI hydrogen station electric demand over a week.

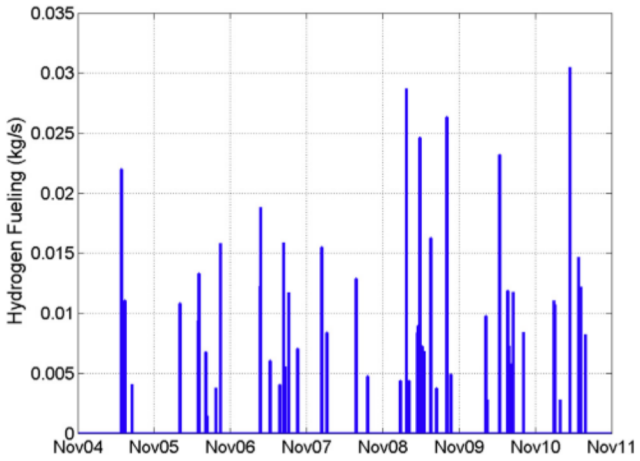

Fig. 3 – UCI hydrogen station hydrogen dispensed over a week.

stack. The PEM electrolyzer cell voltage (V_{cell}) was expressed as equation (1), where E is the open circuit voltage, η_{act} is the activation overpotential, η_{ohm} is the ohmic overpotential and η_{diff} is the diffusion overpotential [21,29]. Using the Nernst equation, the open circuit voltage was calculated by equation (2), where E^0_{rev} is the reversible cell voltage (1.23 V), R is the gas constant, T is the temperature of the electrolyzer; z is the number of moles of electrons transferred per mole of H_2; F is Faraday's constant; P_{H_2},P_{O_2} and P_{H_2O} are the partial pressures of hydrogen, oxygen, and water, respectively [20,30]. The activation overpotential was based on electrochemical reaction kinetics and can be deduced from Butler–Volmer equation and rewritten for an electrolyzer as equation (3), where α is the transfer coefficient and i_0 is the exchange current density [29]. The diffusion overpotential was characterized by equation (5), where β is the constant coefficient and i_{lim} the diffusion limit current density [29]. The limiting current density is taken to be 1.55 A/cm^2 in our model, which is consistent with literature values [29]. The ohmic overpotential was due to the electrical resistances in the electrolyzer cell that are mainly due to proton conduction resistance in the proton exchange membrane. The ohmic overpotential was given by equation (5), where δ_m is the thickness of the membrane, A is the membrane cross-sectional area, σ_m is the conductivity of the proton exchange membrane given by equation (6) proposed by Springer et al. [31], where λ_E is the degree of humidification of the membrane, ranging from 14 (dry enough) to 22 (bathed) [20,21,29,30]. In the case of the PEM electrolyzer, the membrane can be considered to be fully hydrated and in this study, λ_E is assumed to be 17 representing good hydration. According to Faraday's Law, the hydrogen production molar flow rate was given by equation (7), where F is Faraday's constant [20,21,29,30].

$$V_{cell} = E + \eta_{act} + \eta_{ohm} + \eta_{diff} \tag{1}$$

$$E = E^0_{rev} + \frac{RT}{zF}\ln\left(\frac{P_{H_2}P^{1/2}_{O_2}}{P_{H_2O}}\right) \tag{2}$$

$$\eta_{act} = \frac{RT}{\alpha zF}\ln\left(\frac{i}{i_0}\right) \tag{3}$$

$$\eta_{diff} = \frac{RT}{\beta zF}\ln\left(1+\frac{i}{i_{lim}}\right) \quad (4)$$

$$\eta_{ohm} = \frac{\delta_m I}{A\sigma_m} \quad (5)$$

$$\sigma_m = (0.005139\lambda_E - 0.00326)\exp\left[1268\left(\frac{1}{303}-\frac{1}{T}\right)\right] \quad (6)$$

$$n_{H_2} = \frac{I}{2F} \quad (7)$$

In order to verify the PEM electrolyzer model, experimental data from a 6.5 kW (135 A rated, stack voltage = 48 V) PEM electrolyzer stack from NREL's Wind-to-Hydrogen Project were obtained [17]. The electrolyzer model verification can be found in our previous paper [8]. The stack current and voltage were obtained and utilized to verify the developed model operating at 308 K and 190 psi (1310 kPa) and at 328 K and 190 psi (1310 kPa). The simulation of stack voltage efficiency was also compared with experimental data at the operating temperature of 328 K, cathode pressure of 190 psi (1310 kPa), and anode pressure of 30 psi (206.8 kPa). It was shown that the model results agreed well with the experimental data [8]. The tuned PEM electrolyzer model parameters used in the simulation were listed in Table 1. In the hydrogen station model, the stack was scaled up to a rated 300 kW at 135 A (maximum power of 360 kW at 150 A), with 910 electrolysis cells in series operated at 328 K and 200 psi (1379 kPa).

PEMFC model

The PEM fuel cell physical model developed in this study was a similar steady-state model that simulates relations between the cell voltage and cell current that account for activation losses, concentration losses, and ohmic losses. The PEM fuel cell voltage was expressed as equation (8), where E is the open circuit voltage, η_{act} is the activation overpotential, η_{ohm} is the ohmic overpotential and η_{conc} is the concentration overpotential [33,34]. Using the Nernst equation, the open circuit voltage was calculated by equation (9), where E^0_{rev} is the reversible cell voltage, R is the gas constant, T is the temperature of the fuel cell; z is the number of moles of electrons transferred per mole of H_2; F is Faraday's constant; P_{H_2},P_{O_2} and P_{H_2O} are the partial pressures of hydrogen, oxygen, and water, respectively [33,34]. The activation overpotential was based on electrochemical reaction kinetics and can be deduced from Butler–Volmer equation and expressed as equation (10), where α is the transfer coefficient and i_0 the exchange current density. The concentration overpotential was characterized by equation (11), where i_{lim} the limiting current density. The ohmic overpotential was due to the electrical resistances in the fuel cell that was mainly contributed from proton exchange membrane. The ohmic overpotential was given by equation (12), where r_m is the resistivity of the proton exchange membrane, and λ_{FC} is the water content of the membrane [33,34]. Consumption of hydrogen was calculated with Faraday's Law given by equation (7), where n_{H_2} is the number of moles of hydrogen consumed per second.

Table 1 – PEM electrolyzer model parameters.

i_0	Exchange current density	0.0013 A/cm^2 [21]
λ_E	Hydration ratio	17
α	Charge transfer coefficient	0.34
β	Constant coefficient	0.06
δ_m	Membrane thickness	0.04 cm [32]
A	Membrane cross-section area	100 cm^2

Table 2 – PEMFC model parameters.

i_{0_a}	Anode exchange current density	0.00035 A/cm^2
i_{0_c}	Cathode exchange current density	0.0003 A/cm^2
α	Charge transfer coefficient	0.50
t_m	Thickness of the membrane	23 μm [35]
λ_{FC}	Water content	20

$$V_{cell} = E - \eta_{act} - \eta_{ohm} - \eta_{conc} \quad (8)$$

$$E = E^0_{rev} + \frac{RT}{zF}\ln\left(\frac{P_{H_2}P^{1/2}_{O_2}}{P_{H_2O}}\right) \quad (9)$$

$$\eta_{act} = \frac{RT}{\alpha zF}\ln\left(\frac{i}{i_0}\right) \quad (10)$$

$$\eta_{conc} = \frac{RT}{zF}\ln\left(\frac{i_{lim}}{i_{lim}-i}\right) \quad (11)$$

$$\eta_{ohm} = ir_m = i\frac{181.6\left[1+0.03i+0.062\left(\frac{T}{303}\right)^2 i^{2.5}\right]}{(\lambda_{FC}-0.634-3i)\exp\left[4.18\left(\frac{T-303}{T}\right)\right]}t_m \quad (12)$$

In order to verify the PEM fuel cell model, experimental data of a 50 cm^2 single cell were obtained [35]. Two sets of data were obtained and utilized to verify the model developed in this paper, one for operating at 363 K and one for operating at 348 K. The polarization curves presented in our previous paper [8] showed that the model results agreed well with the experimental data. The tuned PEM fuel cell model parameters used in the simulation are listed in Table 2, where i_{0_a} and i_{0_c} are used to calculate the activation losses of anode and cathode, respectively. In the hydrogen station model, the stack was scaled up to 50 kW and operated at 363 K.

Compressor and storage tank model

The hydrogen compressor was modeled with reasonable accuracy by assuming that hydrogen is an ideal gas [18]. The amount of work required to compress hydrogen can be modeled by a polytropic process for the compressor [6,18,19,36] and the mass and energy balances were also calculated using the tank and associated piping as a control volume, as described elsewhere [8].

Assumptions

The following assumptions were made in the system model:

- Wind turbine is a Vestas model V47 that is rated at 50 kW, and 4 wind turbines are employed.
- $\eta_{comp} = 80\%$.
- PEM electrolyzer system is rated at 300 kW, PEM fuel cell system is rated at 50 kW.
- Electrolyzer H_2 outlet pressure is 1379 kPa (200 psi) [17].
- Maximum allowable hydrogen storage tank pressure is 35 MPa (~5000 psi).
- The hydrogen diaphragm compressor could meet the needs of hydrogen compression, is modeled using a polytropic process with n = 1.609, and efficiency, $\eta = 0.8$.
- Volume of the hydrogen storage tank is 10 m^3.
- No inverter/converter losses.
- Sufficient ancillary equipment (e.g., switchgear, inverters and converters, small amount of battery storage for inrush currents) with sufficient ramp rates are available to capture excess wind power dynamics as well as provide enough dynamic power during discharge of storage.

Results and discussion

As stated above, the dynamics of renewable sources and hydrogen fueling are key issues to understand the potential performance of self-sustainable hydrogen fueling stations and their impacts on renewable energy integration into transportation and the utility grid network. Therefore, in this paper, integrated renewable energy powered hydrogen fueling station designs were simulated; analyses using both wind and solar energy sources with various capacity factors were accomplished. In addition, sizing analysis of the station and estimations of the cost of hydrogen were performed.

Control strategies

To compare the station performance, three simple operation and control strategies were implemented in the renewable hydrogen fueling station dynamic model. The control strategies tested are described in Table 3. The key difference among the control strategies implemented is how the station electrical loads are met. The electric power demand of the station is comprised of compressor power demand and station operating/fueling power demand. The electric power is either supplied by the renewable sources directly (when renewable power is available) or by the fuel cell with stored hydrogen as the fuel (when renewable power is not available).

To analyze the implications of the wind intermittency dynamics along with the station operation dynamics, a wind farm with 4 turbines (each rated at 50 kW) was implemented in the self-sustainable hydrogen fueling station system model. Over the course of one week as shown in Fig. 4 (top), the wind power had a relatively high capacity factor of 0.41. It was noted that the wind power was highly dynamic and that daily wind power varied over the week by a factor of 4. Compared to the hydrogen dispensing profile shown in Fig. 3, the wind power profile implemented as shown in Fig. 4 did not exhibit a repeatable diurnal pattern. Large decreases of wind power occurred in the middle of the day for most of the days in this week. Fig. 4 also presents the state of charge (SOC) of the hydrogen storage tank for one week of operation using three different control strategies. The fueling station started operating with the SOC of the storage tank at ~53%. Operating under all three control strategies, the fueling station was able to supply the hydrogen needed for the vehicle refueling while at least maintaining the initial SOC by the end of the week. Operating with control strategies 2 or 3, the amount of hydrogen stored in the storage tank was accumulating during the course of the week. It was noted that control strategy 3 led to the highest SOC (80%) at the end of the week. The dynamics of the production and the consumption, the hydrogen produced from the electrolyzer and consumed in the fuel cell were simulated and presented in our previous study [8].

Table 3 – Control strategies tested.

No.	Control strategy
1	• Use all available renewable power to produce hydrogen • Use fuel cell and stored hydrogen to meet the compressor load, and the station fueling load
2	• Use renewable power captured to produce hydrogen and provide power to compress the hydrogen being produced at the same time • Use fuel cell and stored hydrogen to meet the station fueling load
3	• Use all renewable power captured to meet the load first, if no renewable power is available, use fuel cell with stored hydrogen to meet the station fueling load • Use the rest of the renewable power captured to produce hydrogen and provide power to compress the hydrogen being produced

To analyze the implications of the solar PV power dynamics along with the station operation dynamics, the self-sustainable station was designed with a PV array rated at 360 kW. The solar power profile (with a capacity factor of 0.22) that occurred over the course of one week is shown in Fig. 5 (top). It indicated that the solar power exhibited a very

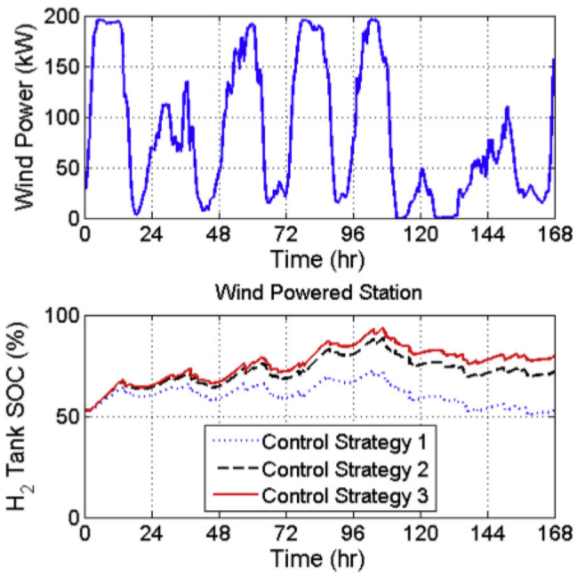

Fig. 4 – (Top) Wind power profile (capacity factor = 0.41), and (Bottom) the state of charge of the hydrogen storage tank for one week operation, station powered by wind.

consistent diurnal pattern with minimal variations over the course of the week. The diurnal characteristic of solar power matched well with the fueling activities of the hydrogen station as shown in Fig. 3, which typically occurred during the day time. Fig. 5 (bottom) presents the SOC of the hydrogen storage tank for the one week of operation using the three control strategies developed, with solar energy as the power source. Similar to the previous wind power cases, the fueling station started operating with the SOC of the storage tank at ~53%. As shown in the results, operating under control strategies 2 and 3, the hydrogen in the storage tank was accumulating throughout the course of the week. Operating under control strategy 3 the fueling station yielded the highest SOC (~72%) at the end of the week. While operated under control strategy 1, the SOC (~49%) at the end of the week was lower than the initial SOC, indicating an imbalance of supply and demand of hydrogen.

To compare the station performance using different renewable energy sources and controls strategies, detailed energy fluxes are shown in Figs. 6 and 7. Over the course of the week simulated, total wind energy input to the hydrogen station is 13,538.5 kWh and total solar energy input is 13,488.2 kWh, with a difference of less than 0.4%. For all cases, the initial hydrogen energy in the storage is 5012.8 kWh (LHV), and the fueling output is 5340 kWh (LHV). Regardless the type of energy sources, the hydrogen fueling station system produced a larger amount of hydrogen and had larger electrolysis losses using control strategy 1. In addition, with control strategy 1, the fuel cell consumed a large amount of hydrogen to power the compressor with unavoidable round trip efficiency penalty. The variations of the fuel cell energy losses and electrolysis losses amongst the control strategies can be observed in Figs. 6 and 7. Operating with control strategy 3, more renewable power was routed to meet the station and compression demand; consequently a lesser amount of hydrogen was produced therefore lesser electrolysis losses

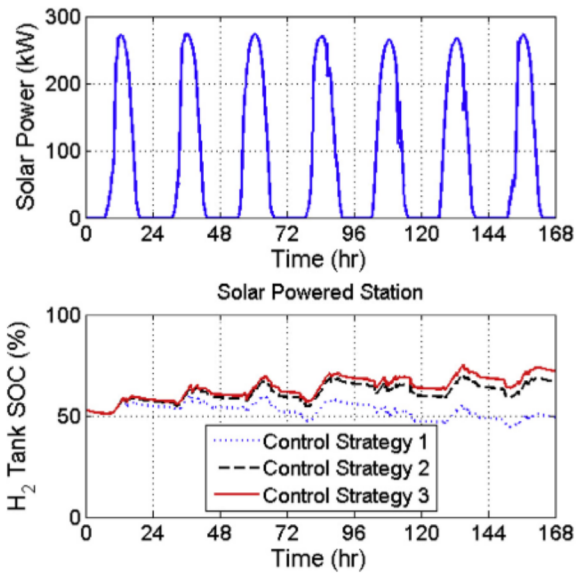

Fig. 5 – (Top) Solar power profile (capacity factor = 0.22), and (Bottom) the state of charge of the hydrogen storage tank for one week operation, station powered by solar PV.

was generated. As opposed to control strategy 1, much less hydrogen was consumed in the fuel cell using control strategy 3. The overall effect of the imbalance of production and consumption led to the fact that the control strategy 3 had the highest yield of hydrogen at the end of the week of operation. Furthermore, the control strategies implemented in combination with the dynamic operating characteristics of the renewable sources determine the amount of hydrogen that is consumed in fuel cell and the amount that is stored in the storage tank. Because of the round trip efficiency penalty associated with converting electricity to hydrogen in an electrolyzer and vice versa in a fuel cell, the results suggest that the station control strategy should utilize the renewable sources directly to power the station equipment whenever it is possible, and keep the hydrogen utilized in the fuel cell as low as possible.

As shown in Figs. 6 and 7, operating with the same control strategy, lower electrolyzer losses and higher yield of hydrogen in the storage were achieved using wind energy sources. This increased yield was due to the higher capacity factor of the wind, which allows it to more often directly provide station power when needed. In addition, the overall energy conversion efficiencies of electrolyzer and fuel cell over the week of operation were summarized in Table 4. The stack efficiency of the PEM electrolyzer was determined by comparing ideal stack potential with actual stack potential [17]. These efficiencies listed were based on the lower heating value (LHV) of hydrogen. The results also indicated that control strategy 3 led to the best station performance among all control strategies simulated.

Impact of capacity factor

The capacity factor of a wind turbine (solar photovoltaic) is its average power output divided by its rated power capability. Capacity factor depends upon device performance and upon the availability of the renewable energy at the device over a period of time. Higher capacity factors imply larger amounts of energy conversion and power generation for any given size of installation. From 1993 to 2012, U.S. offshore wind capacity factors ranged from 0.27 to 0.54, while solar photovoltaic capacity factors ranged from 0.16 to 0.28 [37]. To evaluate the impact of various capacity factors on the performance of the self-sustainable hydrogen fueling station, wind power profiles with relatively low capacity factors of 0.2 and 0.3, solar power profiles with relatively low capacity factors of 0.06 and 0.14 were obtained and evaluated over the course of one week. Control strategy 3, the hydrogen station electrical load and the hydrogen dispensed over the week shown in Figs. 2 and 3 were applied in all of these simulations.

Fig. 8 presents the station performance over the week when the wind power had a capacity factor of 0.3. Around hour 24, 72 and 96 there was no wind power supplied to the station, to maintain the normal operation of the fueling station, hydrogen was required for the fuel cell to provide the power. During the first five days, only a small amount of hydrogen was generated and the storage tank was gradually depleted and reached 25% SOC at the end of fifth day. The simulation results also showed that on the last two days, the storage tank was rapidly filled up when there was a large

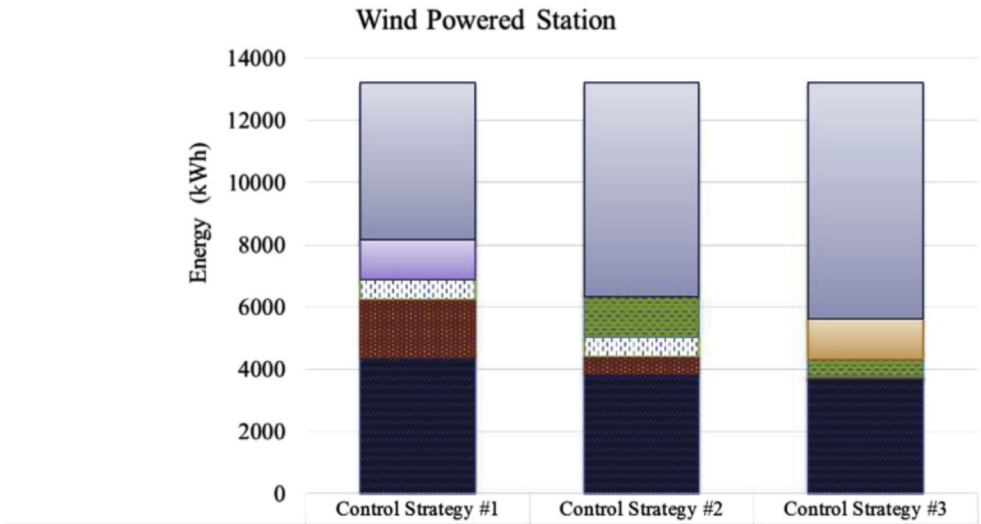

	Control Strategy #1	Control Strategy #2	Control Strategy #3
Hydrogen in the Stroage	5040.26	6878.55	7604.36
Renewable Powered BoP	0.00	0.00	1289.67
Renewable Powered Compressor	0.00	1311.98	539.21
Fuel Cell Powered Compressor	1295.43	0.00	0.00
Fuel Cell Powered BoP	629.01	629.01	47.14
Fuel Cell Losses	1898.38	564.76	42.66
Electrolysis Losses	4348.15	3826.93	3688.18

Fig. 6 – Energy fluxes for wind powered stations using various control strategies.

increase in wind power. The final SOC was greater than the initial SOC, suggesting that the station could manage with this one week of a relative low wind capacity factor while fulfilling all of the fueling demand.

Fig. 9 presents the station performance over the week when the wind power had a capacity factor of 0.2. During the week, 6673 kWh of wind energy was supplied to the station. The final SOC was less than the initial SOC, suggesting that

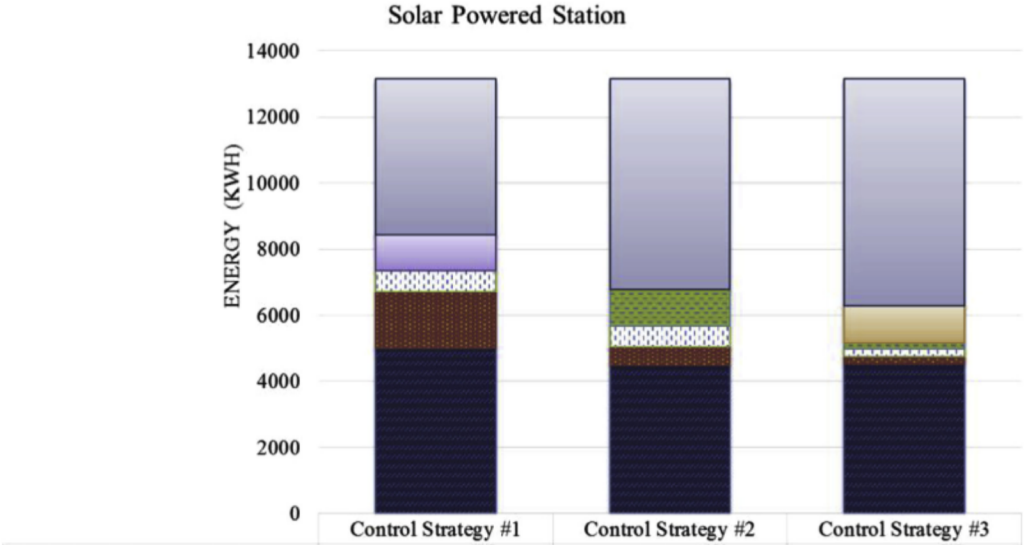

	Control Strategy #1	Control Strategy #2	Control Strategy #3
Hydrogen in the Stroage	4736.37	6376.27	6888.10
Renewable Powered BoP	0.00	0.00	1116.56
Renewable Powered Compressor	0.00	1118.82	179.69
Fuel Cell Powered Compressor	1076.80	0.00	0.00
Fuel Cell Powered BoP	629.01	629.01	239.24
Fuel Cell Losses	1726.59	564.76	210.08
Electrolysis Losses	4992.22	4472.14	4527.32

Fig. 7 – Energy fluxes for solar powered stations using various control strategies.

Table 4 – PEM fuel cell and electrolyzer efficiencies under various scenarios.

		Control strategies		
		C.S.1	C.S.2	C.S.3
Hydrogen station using wind source	PEM fuel cell efficiency	50.34%	52.69%	52.49%
	PEM electrolyzer efficiency	67.88%	68.70%	68.75%
Hydrogen station using solar source	PEM fuel cell efficiency	49.70%	52.69%	53.24%
	PEM electrolyzer efficiency	62.99%	63.85%	63.97%

insufficient hydrogen was generated to maintain the operation of the station.

Fig. 10 presents the station performance over the week when the solar power had a capacity factor of 0.14 with cloudy days in the middle of the week. After one week of operation, the SOC of the storage tank decreased nearly 10%, indicating insufficient production of the hydrogen.

Fig. 11 presents the station performance over the week when the solar power has a very low capacity factor of 0.06 with cloudy days during most of the week. After one week of operation, the SOC of the storage tank decreased sharply to 20%, and most of the fueling and power demands were met by the initial hydrogen storage in the system. Under such conditions and configurations, the hydrogen fueling station can become unsustainable and may fail to meet the fueling load in the following week.

It was also noted that when the station was powered by solar energy sources, large amount of hydrogen was consistently needed to provide the base load of the fueling station during night time (mostly for lighting at the station).

Product conversion and station efficiencies

To compare the fueling station performance under various control strategies and capacity factors, weekly production conversion efficiencies and weekly station efficiencies were calculated as shown in Tables 5 and 6, respectively. Weekly production conversion efficiency is defined as hydrogen production efficiency, where the hydrogen produced in the station is divided by the total renewable energy into the system. Hydrogen station system efficiency was calculated using the total amount of hydrogen dispensed and net remaining in storage, divided by the total energy supplied into the system. As shown in Table 5, regardless of the renewable energy source, control strategy 1 led to the highest production conversion efficiencies. This is simply due to the fact that control strategy 1 uses all the available renewable energy to produce hydrogen instead of powering compressors or BoP (Balance of Plant). It was also noted that under control strategy 3, the weekly production conversion efficiencies increased with

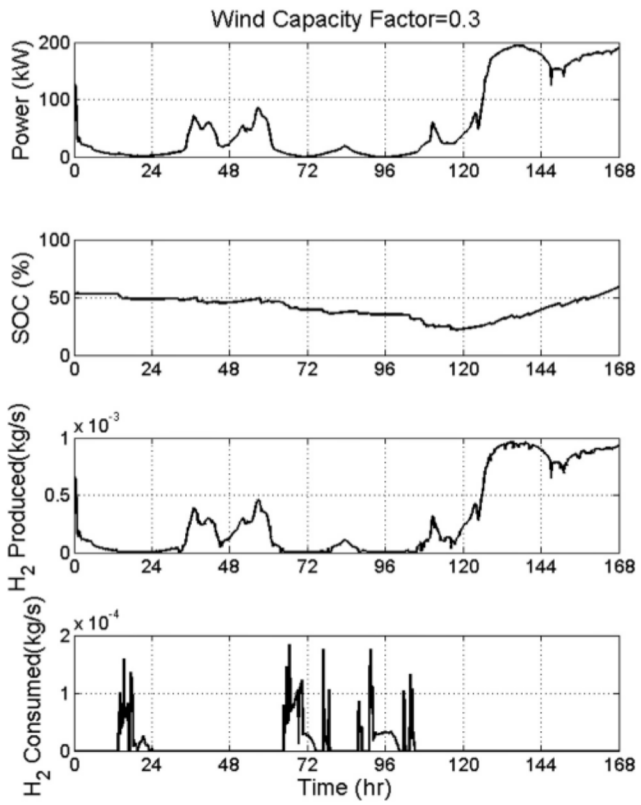

Fig. 8 – Station performance with low wind capacity factor (0.3).

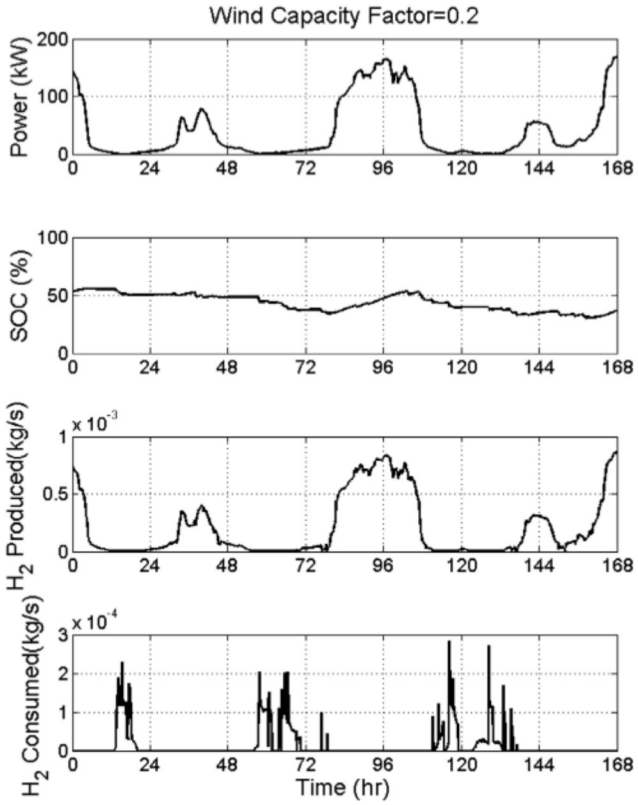

Fig. 9 – Station performance with low wind capacity factor (0.2).

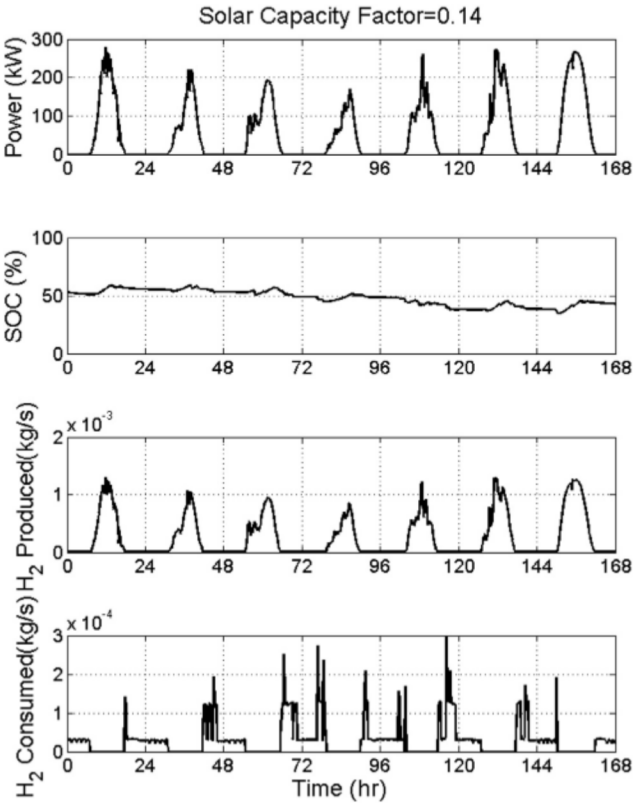

Fig. 10 – Station performance with low solar capacity factor (0.14).

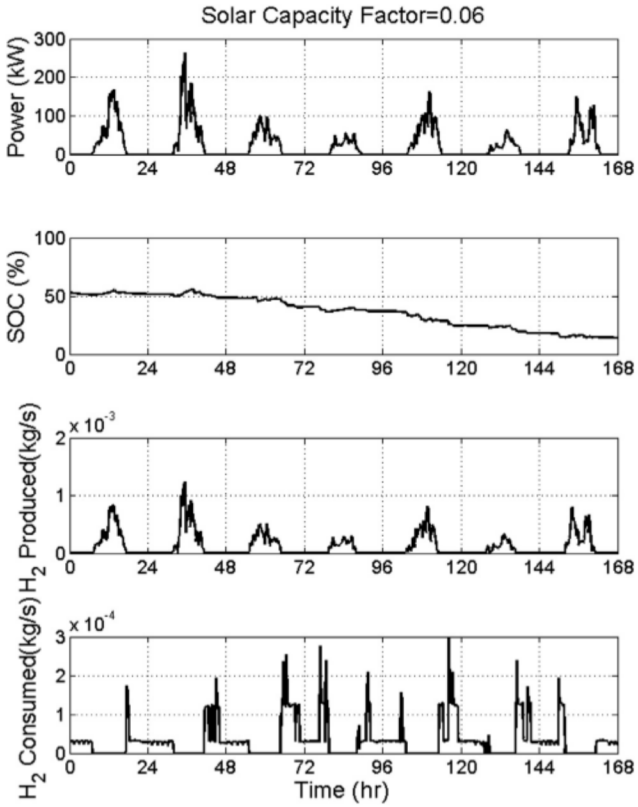

Fig. 11 – Station performance with low solar capacity factor (0.06).

decreasing renewable power capacity factor. Lower capacity factor represents lower power output from the renewable energy sources. Therefore the electrolyzer in the system will operate at the low current region where less loss is associated with hydrogen production. The weekly station efficiency results indicated that the system using control strategy 3 has the highest overall efficiency. With higher capacity factor over the week, higher station efficiency can be achieved.

Impact of energy sources on station sizing

To investigate the implications of the renewable source dynamics on the station design, 52 weeks of wind power and solar power profiles were implemented to the system model independently. In the week long simulations, renewable power profiles of each week over one year were used as input power supply to power the station while the station operation power demand and hydrogen demand (shown in Figs. 2 and 3) were kept the same.

The weekly renewable power magnitudes over an entire year are presented as a boxplot in Fig. 12 using the descriptive statistical method. In this figure, the x-axis represents the week of the year and each of the boxes represents the renewable power recorded over the week. The bottom and top of the box (in blue) are the 25th and 75th percentile levels, and the band (in red near the middle of the box) presents the 50th percentile level. The lower whisker represents the lowest value that within 1.5 IQR (interquartile range) of the lower quartile, and the higher whisker represents the highest value that within 1.5 IQR of the upper quartile. (+) denotes the outliers that are data with values beyond the ends of the whiskers. The spacing between the different parts of the boxes indicates the degree of the dispersion of the data for that week. It can be seen from Fig. 12 that the wind power is highly dynamic and exhibits significant seasonal variations with lowest wind availability in the summer. It is noted that such wind power seasonal variation is typical in the U.S., for both onshore and offshore environments. Typically U.S. wind power potential is greatest in the winter, peaks in January, and is lowest in the summer, with a minimum in August, and varies over the year by a factor of 2 [28,38]. It is also noted that solar power exhibits seasonal variation with a maximum in the summer, and a significantly larger number of outliers can

Table 5 – Weekly production conversion efficiencies under various scenarios.

		Control strategies		
		C.S.1	C.S.2	C.S.3
Hydrogen station using wind energy source	Capacity factor = 0.41	67.9%	62.0%	59.2%
	Capacity factor = 0.30	–	–	60.1%
	Capacity factor = 0.20	–	–	60.7%
Hydrogen station using solar energy source	Capacity factor = 0.22	63.0%	58.5%	56.8%
	Capacity factor = 0.14	–	–	59.4%
	Capacity factor = 0.06	–	–	61.8%

Table 6 – Weekly station efficiencies under various scenarios.

		Control strategies		
		C.S.1	C.S.2	C.S.3
Hydrogen station using wind energy source	Capacity factor = 0.41	39.7%	53.3%	58.7%
	Capacity factor = 0.30	–	–	58.5%
	Capacity factor = 0.20	–	–	56.8%
Hydrogen station using solar energy source	Capacity factor = 0.22	37.5%	49.8%	53.4%
	Capacity factor = 0.14	–	–	53.0%
	Capacity factor = 0.06	–	–	45.4%

be observed indicating an intermittent characteristic of the solar power.

52 weeks of wind power and solar power as shown in Fig. 12 were implemented in the renewable hydrogen station model to determine whether or not the operation and fueling demands shown in Figs. 2 and 3 can be met with various weekly renewable inputs. The hydrogen energy required for station operation and net hydrogen yield over one week for all cases are presented in Figs. 13 and 14. As shown in Fig. 13, the higher the weekly average power of the renewable sources, the lesser the amount of the hydrogen that was required by the fuel cell to supply power for the station operation. For the wind powered station, it was observed that when the weekly average wind power was greater than 150 kW, no hydrogen was required for powering the station in most of the cases. It is also noted that operating under the same weekly average power, the solar powered station required more hydrogen for station operation, mainly due to the fact that hydrogen is required by the fuel cell to provide the base load of the fueling station during night time. The net hydrogen yield after one week of operation using various renewable sources is presented in Fig. 14. Not surprisingly, higher weekly average renewable power had higher net hydrogen yield after one week of operation. To dispense 24 kg of hydrogen over the week and break even at the end of the week, the minimum weekly average wind power and solar power were 54.6 kW and 60.3 kW, respectively. It was also observed that operating under the same weekly average power, the solar powered

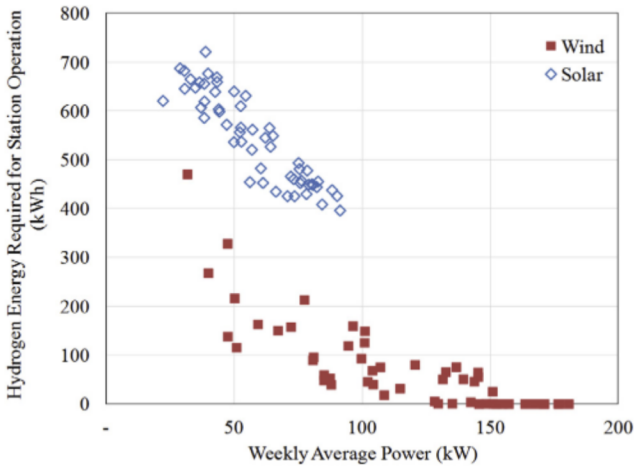

Fig. 13 – Hydrogen energy required for station operation over one week using various renewable power supplies.

station yielded less hydrogen over the week, mainly due to the fact that hydrogen has to be consumed during night time to provide the base load of the fueling station.

To provide insights on the design of self-sustainable renewable hydrogen fueling stations, the impact of renewable rated power and capacity factor on the weekly hydrogen net yield was evaluated and is presented in Figs. 15 and 16. For this analysis, the station was designed to dispense 24 kg of hydrogen over the week. As indicated in Figs. 15 and 16, to achieve this design point, the station needed to be designed above the zero net yield line. The results indicated that the siting of the self-sustainable hydrogen fueling station will determine the size of the wind turbine and solar PV needed. Given the fixed amount of hydrogen dispensed per week, the higher weekly average capacity factor of the renewable sources at the area where the station sited, the smaller wind turbine/solar PV is required. The results also provided insights on the sizing of hydrogen storage tank and maximum fueling capacity of the station. For example, for the specific week of fueling station operation, a 200 kW wind turbine installed at

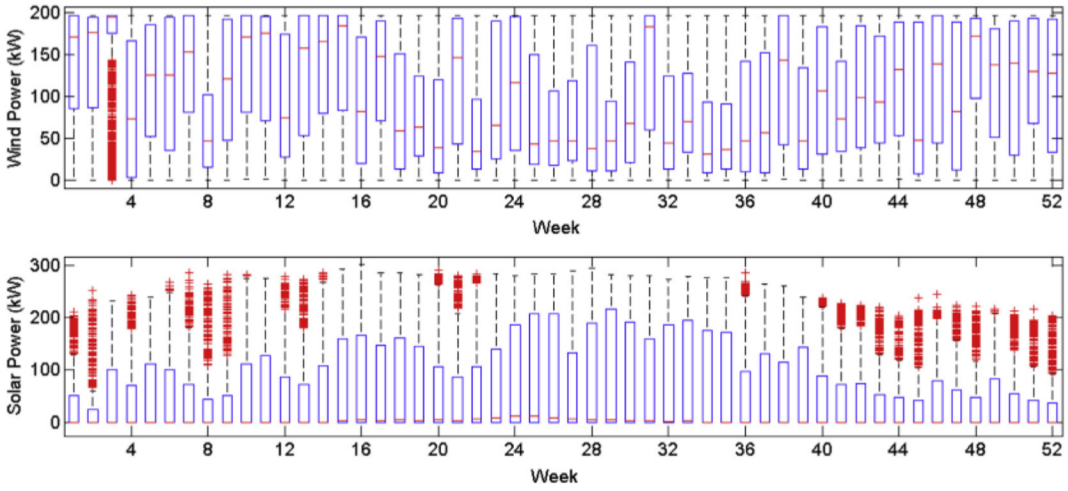

Fig. 12 – Boxplot of weekly wind and solar power over one year.

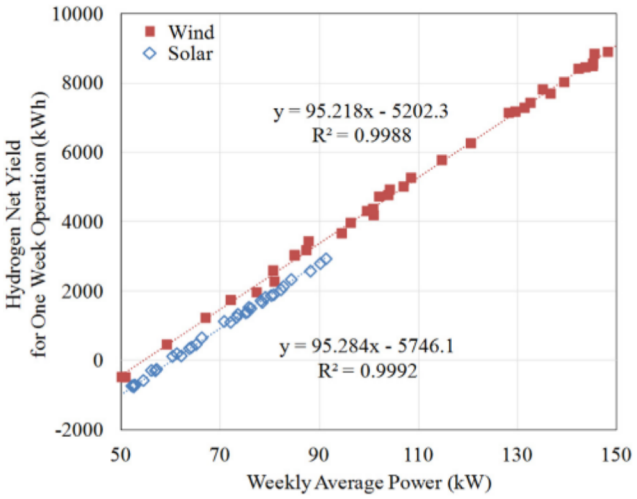

Fig. 14 – Hydrogen net yield for one week operation using various renewable power supplies.

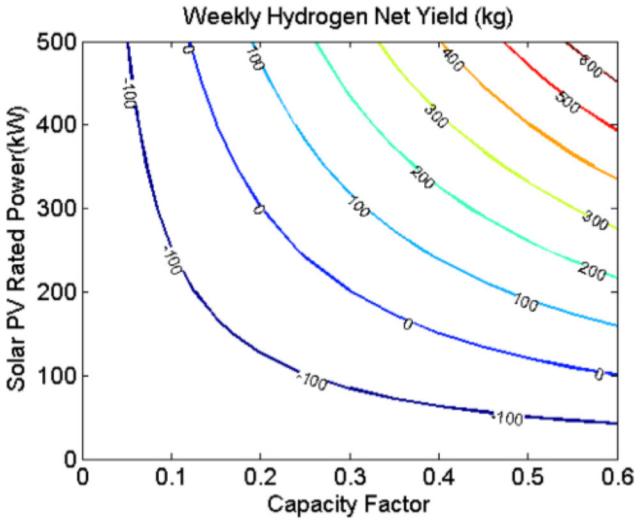

Fig. 16 – Change in weekly hydrogen net yield with various solar PV rated power and capacity factor.

the station where weekly average wind capacity factor of 0.5 will have a net yield of over 100 kg hydrogen at the end of the week. Under the same wind condition and fueling activities, a station with 150 kW wind turbine installed will have a net yield of about 50 kg hydrogen at the end of the week. To maintain a balance between production and consumption and at least achieve zero net yield at the end of the week, the solar powered station requires larger PV capacity installed. With solar capacity factor of 0.15, at least 400 kW solar PV has to be installed in the station to support the fueling activities during the week.

Cost of hydrogen and sensitivity analysis

To evaluate the feasibility of the self-sustainable hydrogen fueling station, the cost of hydrogen was evaluated based upon the station model developed in this study. The per kg

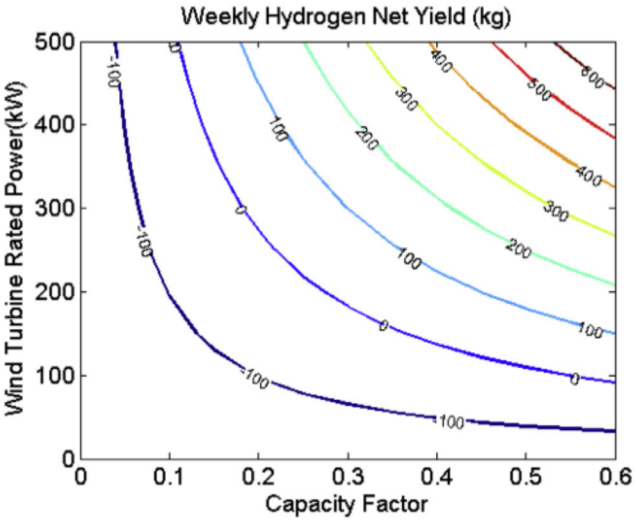

Fig. 15 – Change in weekly hydrogen net yield with various wind turbine rated power and capacity factor.

cost of hydrogen was estimated based upon factors including control strategy, capacity factor, levelized renewable energy cost, levelized cost of PEM fuel cell and electrolyzer, compressor, storage, dispenser and BoP of the fueling station. The detailed hydrogen production cost contributions are presented in Table 7. Levelized cost is defined as total costs (including annualized capital and yearly operating costs) divided by total energy service production (kg of fuel produced or kWh of electrical energy produced). The cost of a net 80-kW PEM fuel cell system based on 2012 technology and operating on direct hydrogen was projected to be $84/kW when manufactured at a volume of 10,000 units per year [39]. The cost of a 50 kW PEM fuel cell system with 10,000 h lifetime was evaluated based on these values.

Based upon the cost contribution and the medium costs of Table 7, powered by a 200 kW wind turbine and operated using control strategy 3, the cost of hydrogen is $8.01 per kg. On the other hand, using a 360 kW PV array and operated using control strategy 3, the cost of hydrogen is $20.22 per kg. According to the U.S. Department of Energy, the cost of centralized or distributed hydrogen production from wind has 2015 targets of $3.10/kg and $3.70/kg, respectively [25]. However, the costs of hydrogen produced by the self-sustainable hydrogen fueling station simulated in this study using the lower end costs of Table 7 lead to$6.71/kg-$H_2$ for the wind powered station and $9.14/kg-$H_2$ for the solar powered station. Note that these hydrogen costs are comparable to the cost of hydrogen dispensed at the current UCI hydrogen fueling station ($14.94/kg-$H_2$) [1]. Note also, that the self-sustainable hydrogen fueling station produces and dispenses the hydrogen without any additional cost for transporting the hydrogen, or compressing and dispensing the hydrogen.

Single-factor cost sensitivity analysis was carried out to evaluate the effects of several variables on the cost of hydrogen. Single-factor analysis evaluates the effect on the outcome of each factor one at a time, while keeping the other factors at their base value. Table 7 showed the variable,

Table 7 – Hydrogen production cost contribution.

	Levelized energy cost ($/kWh)		Levelized capital cost ($/kWh)	Levelized hydrogen cost ($/kg-$H_2$)	
	Wind [25,26,40,41]	Solar PV [40]	PEM fuel cell [39]	PEM electrolyzer [42]	
Low	0.090	0.103	0.275	0.300	
Medium	0.100	0.280	0.42	0.700	
High	0.110	0.360	1.09	1.200	
	Levelized cost, portion of compressor, storage, and dispensing ($/kg-$H_2$) [41,43]				
	Compressor	Storage	Dispenser	Refrigeration	Remainder of Station	Total
Low	0.191	0.825	0.083	0.115	0.008	1.222
Medium	0.498	0.825	0.083	0.115	0.008	1.529
High	0.804	0.825	0.083	0.115	0.008	1.835

medium value and the high and low values of each variable obtained from various sources. Fig. 17 presented the cost sensitivity of hydrogen produced from a wind powered fueling station. Low to high cost ranges of each variable were shown in the Tornado diagram. The results clearly showed that wind energy cost was the most important variable, followed by electrolyzer cost, and then by compressor, storage and dispensing cost. Fuel cell cost only had a minor impact on the hydrogen cost. In addition, the base cost ($8.01/kg-$H_2$) was calculated based upon 40% capacity factor, therefore the quality of the wind resources at the particular hydrogen station site will also have significant impact on the cost of hydrogen. Each self-sustainable hydrogen fueling station powered with wind energy will have unique characteristics based upon average yearly wind speed and capacity factor, which will lead to various hydrogen costs for each station. It was also noted that the fuel cell had the least impact on the overall cost of hydrogen since a relatively small PEM fuel cell was required in the system.

Fig. 18 presents the cost sensitivity of hydrogen produced from a solar powered fueling station. The results show that the solar energy cost has the dominant impact and contributed the most to the variability of the cost of the hydrogen. The base cost ($20.22/kg-$H_2$) was calculated based upon the average levelized energy cost ($0.28/kWh) of solar PV systems determined from a survey of 44 installations in the 2007 to 2012 timeframe [40]. However, using the 2012 PV cost estimation from DOE ($0.103) [40] the cost of hydrogen is determined to be as low $9.14 per kg for the PV powered station. The two primary drivers of levelized energy cost of the solar PV electricity are energy production in kWh and system cost, therefore in a region with good annual solar insolation such as the Mojave Desert (7.7 kWh/m^2/day compared to the U.S average 4.1 kWh/m^2/day), the levelized energy cost of solar PV is significantly lower. As a result, a solar PV powered hydrogen station installed in a remote area, such as the High Desert Corridor of California where hydrogen delivery is otherwise challenging and expensive, will have lower hydrogen cost.

Station component design

The constraints needed to be considered in designing a self-sustainable hydrogen fueling station include location, renewable energy source availability, fueling demand and cost of hydrogen. Using the method discussed in section 'Impact of Energy Sources on Station Sizing', the capacity factors of the renewable sources can be obtained via historical wind/solar data and used as guideline to sizing the wind turbine/solar array with a chosen location and fixed fueling capacity. The size of the electrolyzer system can be then determined by the combination of the rated power of the wind turbine/solar array and the renewable capacity factors. Based upon the fueling capacity, the base electric load of the station can be estimated and as a result the size of the fuel cell can be determined. The hydrogen compressor and the size of the storage tank can be estimated by the size of the electrolyzer, average renewable power and the maximum fueling capacity. As discussed in the previous section, the cost of hydrogen will depend upon the renewable energy sources and the system components. The self-sustainable

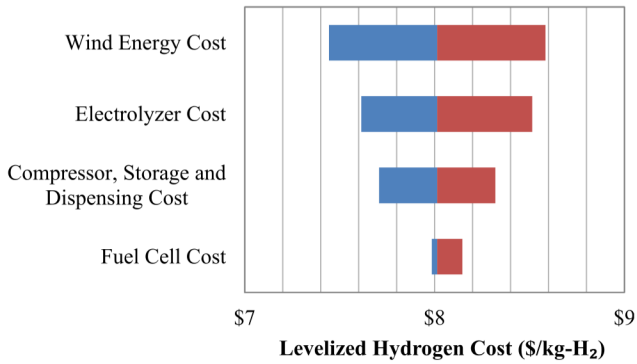

Fig. 17 – Cost sensitivity for hydrogen produced in the wind powered fueling station.

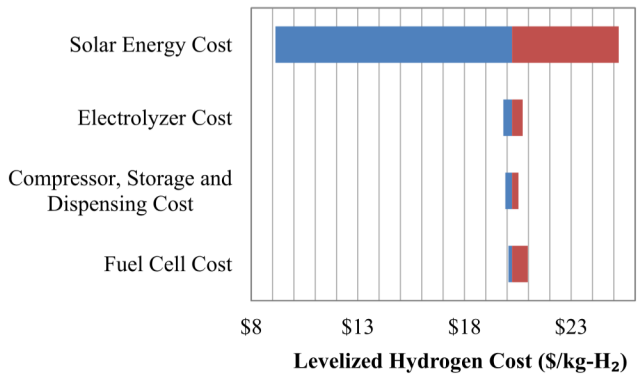

Fig. 18 – Cost sensitivity for hydrogen produced in the solar powered fueling station.

hydrogen station model developed in this study could provide guidelines for the system design and optimization.

Summary and conclusions

For the purpose of investigating the feasibility and dynamic performance of a self-sustainable hydrogen fueling station solely using renewable energy sources, system models were developed to simulate a wind farm, solar array and hydrogen fueling station with PEM electrolyzer and fuel cell. The fueling dynamics and power consumption dynamics were obtained from an operating public hydrogen fueling station and implemented in the system model. Various control strategies were simulated and the station performance was determined based upon the dynamics of renewable power and how it was utilized in the station. Because of the round trip efficiency penalty associated with converting electricity to hydrogen (in an electrolyzer) and vice versa (in a fuel cell), the results suggest that the station operation power should be supplied by the renewable sources directly whenever possible, and that the hydrogen fuel cell should provide power only when there is no renewable power available. The simulated hydrogen fueling station powered by 200 kW wind turbines or 360 kW solar PV were determined to be able to successfully operate in a self-sustainable manner while dispensing ~25 kg of hydrogen per day. The impact of the renewable power capacity factor on the station operation was also evaluated. For lower capacity factor, a larger amount of renewable energy conversion devices is required to ensure continuous operation of the fueling station. 52 weeks of various renewable power dynamics were implemented in the system model to investigate the implications of the renewable source dynamics on the station design and performance. A guideline to determine the amount of renewable capacity installed in the station based upon the renewable capacity factors is provided. Furthermore, this study provides insights regarding the sizing of the station components such as the renewable energy conversion devices, electrolyzer and fuel cell, and storage tank. The cost of the hydrogen was estimated and can be as low as $6.71 per kg when the station was powered by 200 kW of wind turbines and operated using control strategy 3, while the cost increased to $9.14 per kg when the station was powered by 360 kW of PV arrays and operated using control strategy 3. Sensitivity analyses suggested that the renewable energy cost was the most important cost variable.

This study provides a basis for achieving self-sustainable renewable hydrogen fueling stations. With further optimization, these self-sustainable renewable hydrogen fueling stations could provide valuable interconnections (especially in remote locations) throughout the hydrogen infrastructure network and further support the integration of renewable sources for vehicle fuels.

Acknowledgments

The authors would like to thank Prof. Scott Samuelsen, Dr. Tim Brown, Mr. Richard Hack, and Ms. Jean Grigg from Advanced Power and Energy Program, University of California, Irvine, for their technical support.

REFERENCES

[1] Brown T, Stephens-Romero S, Scott Samuelsen G. Quantitative analysis of a successful public hydrogen station. Int J Hydrog Energy 2012;37:12731–40.
[2] Balat M. Potential importance of hydrogen as a future solution to environmental and transportation problems. Int J Hydrog Energy 2008;33:4013–29.
[3] Dunn S. Hydrogen futures: toward a sustainable energy system. Int J Hydrog Energy 2002;27:235–64.
[4] Veziroglu A, Macario R. Fuel cell vehicles: state of the art with economic and environmental concerns. Int J Hydrog Energy 2011;36:25–43.
[5] Lee J-Y, An S, Cha K, Hur T. Life cycle environmental and economic analyses of a hydrogen station with wind energy. Int J Hydrog Energy 2010;35:2213–25.
[6] Dursun E, Acarkan B, Kilic O. Modeling of hydrogen production with a stand-alone renewable hybrid power system. Int J Hydrog Energy 2012;37:3098–107.
[7] Kelly N, Gibson T, Ouwerkerk D. A solar-powered, high-efficiency hydrogen fueling system using high-pressure electrolysis of water: design and initial results. Int J Hydrog Energy 2008;33:2747–64.
[8] Zhao L, Brouwer J, Scott Samuelsen G. Dynamic analysis of a self-sustainable renewable hydrogen fueling station. In: Proceedings of the ASME 2014 8th international conference on energy sustainability & 12th fuel cell science, engineering and technology conference. Boston, Massachusetts: ASME; 2014.
[9] Farzaneh-Gord M, Deymi-Dashtebayaz M, Rahbari HR, Niazmand H. Effects of storage types and conditions on compressed hydrogen fuelling stations performance. Int J Hydrog Energy 2012;37:3500–9.
[10] Shah A, Mohan V, Sheffield JW, Martin KB. Solar powered residential hydrogen fueling station. Int J Hydrog Energy 2011;36:13132–7.
[11] Dagdougui H, Ouammi A, Sacile R. Modelling and control of hydrogen and energy flows in a network of green hydrogen refuelling stations powered by mixed renewable energy systems. Int J Hydrog Energy 2012;37:5360–71.
[12] Rothuizen E, Mérida W, Rokni M, Wistoft-Ibsen M. Optimization of hydrogen vehicle refueling via dynamic simulation. Int J Hydrog Energy 2013;38:4221–31.
[13] Gahleitner G. Hydrogen from renewable electricity: an international review of power-to-gas pilot plants for stationary applications. Int J Hydrog Energy 2013;38:2039–61.
[14] Princerichard S, Whale M, Djilali N. A techno-economic analysis of decentralized electrolytic hydrogen production for fuel cell vehicles. Int J Hydrog Energy 2005;30:1159–79.
[15] Gibson T, Kelly N. Optimization of solar powered hydrogen production using photovoltaic electrolysis devices. Int J Hydrog Energy 2008;33:5931–40.
[16] Calderón M, Calderón AJ, Ramiro A, González JF, González I. Evaluation of a hybrid photovoltaic-wind system with hydrogen storage performance using exergy analysis. Int J Hydrog Energy 2011;36:5751–62.
[17] Harrison KW, Martin GD, Ramsden TG. The wind-to-hydrogen project: operational experience, performance testing, and systems integration. Colorado: Golden; 2009.
[18] Deshmukh SS, Boehm RF. Review of modeling details related to renewably powered hydrogen systems. Renew Sustain Energy Rev 2008;12:2301–30.

[19] Carapellucci R, Giordano L. Modeling and optimization of an energy generation island based on renewable technologies and hydrogen storage systems. Int J Hydrog Energy 2012;37:2081–93.
[20] Awasthi a, Scott K, Basu S. Dynamic modeling and simulation of a proton exchange membrane electrolyzer for hydrogen production. Int J Hydrog Energy 2011;36:14779–86.
[21] Marangio F, Santarelli M, Cali M. Theoretical model and experimental analysis of a high pressure PEM water electrolyser for hydrogen production. Int J Hydrog Energy 2009;34:1143–58.
[22] Maclay J, Brouwer J, Scottsamuelsen G. Dynamic analyses of regenerative fuel cell power for potential use in renewable residential applications. Int J Hydrog Energy 2006;31:994–1009.
[23] Maclay JD, Brouwer J, Samuelsen GS. Dynamic modeling of hybrid energy storage systems coupled to photovoltaic generation in residential applications. J Power Sources 2007;163:916–25.
[24] Maclay JD, Brouwer J, Samuelsen GS. Experimental results for hybrid energy storage systems coupled to photovoltaic generation in residential applications. Int J Hydrog Energy 2011;36:12130–40.
[25] Saur G, Ainscough C. U. S. Geographic analysis of the cost of hydrogen from electrolysis. Colorado: Golden; 2011.
[26] Saur G, Ramsden T. Wind electrolysis: hydrogen cost optimization. Colorado: Golden; 2011.
[27] Kim E, Park J, Cho JH, Moon I. Simulation of hydrogen leak and explosion for the safety design of hydrogen fueling station in Korea. Int J Hydrog Energy 2013;38:1737–43.
[28] Maton J-P, Zhao L, Brouwer J. Dynamic modeling of compressed gas energy storage to complement renewable wind power intermittency. Int J Hydrog Energy 2013;38:7867–80.
[29] Lebbal ME, Lecœuche S. Identification and monitoring of a PEM electrolyser based on dynamical modelling. Int J Hydrog Energy 2009;34:5992–9.
[30] Gorgun H. Dynamic modelling of a proton exchange membrane (PEM) electrolyzer. Int J Hydrog Energy 2006;31:29–38.
[31] Springer TE, Zawodzinski TA, Gottesfeld S. Polymer electrolyte fuel cell model. J Electrochem Soc 1993;138:2334–42.
[32] Ni M, Leung MKH, Leung DYC. Energy and exergy analysis of hydrogen production by a proton exchange membrane (PEM) electrolyzer plant. Energy Convers Manag 2008;49:2748–56.
[33] Kuo J-K, Wang C-F. An integrated simulation model for PEM fuel cell power systems with a buck DC–DC converter. Int J Hydrog Energy 2011;36:11846–55.
[34] Musio F, Tacchi F, Omati L, Gallo Stampino P, Dotelli G, Limonta S, et al. PEMFC system simulation in MATLAB-Simulink® environment. Int J Hydrog Energy 2011;36:8045–52.
[35] Ahluwalia RK, Lajunen XWA, Wang X, Kumar R. Fuel cells systems analysis, 2012. Washington, DC: DOE Hydrogen Program Review; 2012.
[36] Raju M, Khaitan SK. System simulation of compressed hydrogen storage based residential wind hybrid power systems. J Power Sources 2012;210:303–20.
[37] Transparent cost database/open energy information. http://en.openei.org/apps/TCDB/.
[38] Lu X, McElroy MB, Kiviluoma J. Global potential for wind-generated electricity. Proc Natl Acad Sci U S A 2009;106:10933–8.
[39] Spendelow J, Marcinkoski J. DOE fuel cell technologies program record: fuel cell system cost. 2012. p. 1–6.
[40] Transparent cost database/open energy information.
[41] Genovese J, Harg K, Paster M, Turner J. Current (2009) state-of-the-art hydrogen production cost estimate using water electrolysis independent review. Colorado: Golden; 2009.
[42] Hamdan M. 2012 hydrogen program annual merit review meeting: PEM electrolyzer incorporating an advanced low cost membrane. 2012.
[43] DOE H2A production analysis. 2012. http://www.hydrogen.energy.gov/h2a_production.html-http://www.hydrogen.energy.gov/ha_production.html.